http://dx.doi.org/10.5935/0103-5053.20130300

J. Braz. Chem. Soc., Vol. 25, No. 2, 320-330, 2014.
Printed in Brazil - ©2014 Sociedade Brasileira de Química
0103 - 5053 $6.00+0.00

Article

Biopolymer-Clay Nanocomposites: Cassava Starch and Synthetic Clay Cast Films

Gustavo F. Perotti,[a] Jairo Tronto,[b] Marcos A. Bizeto,[c] Celly M. S. Izumi,[d] Marcia L. A. Temperini,[a] Ademar B. Lugão,[e] Duclerc F. Parra[e] and Vera R. L. Constantino*[,a]

[a]Departamento de Química Fundamental, Instituto de Química, Universidade de São Paulo, Av. Lineu Prestes 748, 05508-000 São Paulo-SP, Brazil

[b]Universidade Federal de Viçosa, Instituto de Ciências Exatas e Tecnológicas, Campus de Rio Paranaíba, Rodovia MG-230, km 7, 38810-000 Rio Paranaíba-MG, Brazil

[c]Departamento de Ciências Exatas e da Terra, Instituto de Ciências Ambientais, Químicas e Farmacêuticas, Universidade Federal de São Paulo, Rua São Nicolau, 210, 09913-030 Diadema-SP, Brazil

[d]Núcleo de Espectroscopia e Estrutura Molecular, Departamento de Química, Universidade Federal de Juiz de Fora, 36036-900 Juiz de Fora-MG, Brazil

[e]Centro de Química e Meio Ambiente, Instituto de Pesquisas Energéticas e Nucleares, Av. Lineu Prestes 2242, 05508-900 São Paulo-SP, Brazil

Nanocompósitos à base de amido de mandioca, argila sintética hectorita e açúcar invertido (plastificante) foram preparados por processo em meio aquoso (*casting*) produzindo filmes transparentes e homogêneos. Pequenas quantidades de argila (5-15% em massa) produzem principalmente nanocompósitos esfoliados, enquanto grandes quantidades (30% em massa) promovem a formação de nanocompósitos intercalados. Os espectros FT-Raman mostram que bandas sensíveis à ligação de hidrogênio em grânulos de amido são progressivamente deslocadas para frequências menores quando o teor de argila é aumentado. Os nanocompósitos mostram um comportamento térmico semelhante até 320 °C, enquanto a decomposição da biomolécula em cerca de 500 °C é dependente do teor de argila. A liberação de CO_2 em aproximadamente 300 °C (decomposição não oxidativa das cadeias poliméricas) diminui se comparada com o desprendimento desse gás em 500 °C quando a quantidade de argila é aumentada. Filmes com teor de argila maior que 10% não mostram melhora substancial nas propriedades de alongamento ou resistência.

Polymer-clay nanocomposites (PCN) based on cassava starch, synthetic hectorite clay and inverted sugar cane syrup (plasticizer) were prepared by solvent-assisted (*casting*) process producing transparent and homogeneous films. Small amounts of clay (5-15 wt.%) resulted mainly in exfoliated nanocomposites while large amounts (30 wt.%) promote the intercalated nanocomposites formation. FT-Raman bands sensitive to hydrogen bonding in starch granules are progressively shifted to lower wavenumbers as the clay content is raised. Nanocomposites show a similar thermal behavior up to 320 °C while the biomolecule decomposition at about 500 °C is dependent on the clay content. CO_2 release at about 300 °C (non-oxidative decomposition of polymeric chains) decreases if compared to the gas delivery at ca. 500 °C, as the clay content is increased. Films with clay content higher than 10 wt.% show no substantial benefit for either elongation or resistance properties.

Keywords: nanocomposites, clays, starch, cassava, layered silicates, laponite

*e-mail: vrlconst@iq.usp.br

Introduction

Polymer-clay nanocomposites (PCN) based on the assembly between polymers and layered nano-sized inorganic fillers have received considerable worldwide attention over the last twenty years.[1-8] In such materials, the synergistic interaction between the organic and inorganic phases may give rise to materials with new properties that are not present in the individual pristine parts. The polymer-filler interaction at nanoscale is mainly promoted by the high interfacial area between them, leading to composite materials with enhanced properties such as increased mechanical properties, and improved thermal stability, scratch and damage resistance, gas barrier and flame retardancy.

Particularly, many composites have been prepared through the combination of synthetic polymers and randomly and homogeneously dispersed clay minerals (hydrous layer silicates) of the smectite group (montmorillonite, hectorite, and saponite), that comprise platelet-type materials classified as 2:1 phyllosilicates.[9-14] Several studies were effectively motivated by the works published from Toyota Central R&D Labs in Japan about the Nylon 6 polymerization in the presence of layered silicate.[4] Both mechanical and thermal properties of the Nylon 6-clay greatly increased after introduction of small amounts of clay mineral. One of the most important advantages of the formation of nanocomposite is that only a low quantity of clay is added (3-8 wt.%) when compared to conventional or microcomposites (40-50 wt.%) resulting in superior and lighter materials at low costs of production.

The use of synthetic clays such as Laponite, a hectorite of composition $Na_{0.7}[(Mg_{5.5}Li_{0.4})Si_8O_{20}(OH)_4]$,[15] has many advantages over natural clays as for instance the absence of impurities (silica, iron oxides, carbonates etc.) and well defined chemical formula. This synthetic clay has been employed in diverse fields such as surface coatings, paper and polymer films, agriculture, household and personal care products.[16] A very interesting recent work shows that Laponite is cytocompatible (at concentration < 1 mg mL^{-1}) and a bioactive material for osteogenic differentiation of human mesenchymal stem cells *in vitro*.[17]

Laponite particle shows a disk-like shape. Its relative small size (usually around 25-30 nm in diameter and 1 nm in thickness, Figure 1A),[18,19] combined with its great ability to form transparent colloidal dispersions, facilitates the obtaining of homogeneous polymer-clay nanocomposites by casting method.[20] The Laponite estimated surface area is up to 370 $m^2 g^{-1}$,[21] which can endorse efficient interactions with species in its surroundings. Smectite clay primary particle is a set of negative charged layers arranged face to face and intercalated with hydrated cations to bring about a zero net electric charge. As montmorillonite or saponite, each Laponite layer is formed by the condensation of three sheets (Figure 1A). The denominated *tetrahedral sheet* presents continuous corner-shared tetrahedral [SiO_4] units arranged in hexagonal rings. Connected to two tetrahedral sheets, there is an *octahedral sheet* composed by bivalent or trivalent cations sharing the edges coordinated to hydroxyl groups. In the case of Laponite, octahedral sheet supports Mg^{2+} ions which are partially substituted by Li^+ ions.[22-24]

Several synthetic routes have been used to prepare polymer-clay nanocomposites (PCN): (a) exfoliation-adsorption, (b) *in situ* intercalative polymerization, (c) melt intercalation, (d) template synthesis.[5] Depending on the nature of the organic and inorganic components (and also of the preparation method), three types of PCN can be obtained: conventional or microcomposite, intercalated nanocomposite and exfoliated nanocomposite (Figure 1B).

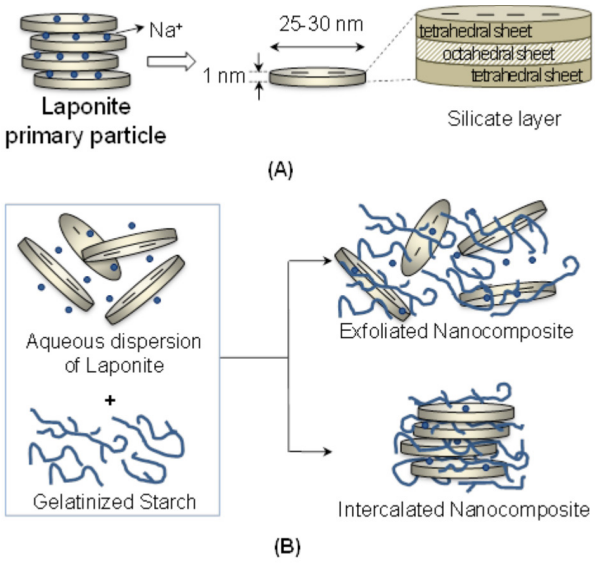

Figure 1. (A) Schematic structure of synthetic Laponite clay; (B) different types of nanocomposites formed by combining polymer and clay particles.

More recently, some studies have reported the preparation and characterization of nanocomposites based on biodegradable polymer from renewable sources and clays.[25,26] These hybrids based on clays, also called *green nanocomposites*, are considered as a new generation of materials. They are attractive to replace the existing petroleum-based plastics with the advantage of being produced from renewed sources and exhibit good biocompatibility and degradability. Some examples of biodegradable polymers include polylactide (PLA),[27] poly(3-hydroxybutyrate) (PHB),[28] chitosan,[29] etc.

Nanocomposites based on biodegradable polymers and layered materials can be used to develop drug delivery

systems for application in medicine and pharmacology.[30] The kinetics of release of bioactive species immobilized on clay particles dispersed in a polymer can be modified; in addition clay nanoparticles can alter the polymer mechanical properties, its ability to swell, and/or its bioadhesion. A very interesting study was reported about a composite based on a chemotherapic drug, montmorillonite clay and a biodegradable polymer.[31] The oral administration of one dose of the nanocomposite supported the anticancer agent delivery for about three weeks in contrast with 22 h for the intravenous administration of a commercial formulation of the drug.

In nature, starch granules are composed by two distinct macromolecules, a linear polymer called amylose and a branched one, known as amylopectin, that coexist in different amounts and form different packing structures depending on the starch source.[32,33] The amylopectin/amylose ratio changes considerably according to the variety of the tuber, normally ranging from 20-30% to 70-80%, respectively.[34] While amylose is formed by D-glucopyranose units bonded in α (1→4) position and shows a counterclockwise helical structure known as V-type,[35] amylopectin also presents α (1→6) bonds on every 20-25 linear units.[36] The representative structures of amylose and amylopectin are shown in Figure 2.

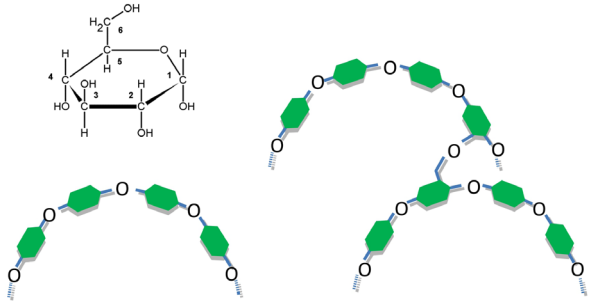

Figure 2. Molecular structure of α-glucopyranose (top left), amylose (bottom left) and amylopectin (right).

The semicrystalline structure of starch granules is well-known by its hierarchical organization and a relative low level of crystallinity, usually ranging from 15 to 45%. Its structure is highly dependent on amylopectin packing, the main component of starch sources with exception of a few maize varieties and some tubers with high amylose content.[32] The three crystalline patterns observed for starches in nature are classified as type-A, obtained from cereal sources such as rice, wheat and cassava, exhibiting a monoclinic lattice.[37] The second one, called type-B is found in many tubers such as potato and presents a hexagonal lattice, while the last form, designed as type-C is most common in seeds and legumes and is actually a mixture of type A and B.[32,38]

Cassava (*Manihot esculenta*) is an interesting source of starch for the development of nanocomposites from biopolymers, especially due to the vast production of this root in many tropical countries, such as Brazil, according to Food and Agriculture Organization of the United Nations (FAO).[39] Besides, the cost associated to the crop and processing of cassava in order to obtain starch is low.

Inverted sugar cane syrup, a mixture of glucose and fructose obtained by sucrose (regular sugar) decomposition, has a low price when compared with other plasticizers such as polyethylene glycol (PEG), and presents the same chemical nature of starch. Hence, it could be used to decrease the interactions among the starch chains, especially the hydrogen bonds, yielding malleable films.[40] Inverted sugar cane syrup also comes from a renewable source obtained from large crops, especially in tropical countries.

This work reports the preparation and characterization of nanocomposites based on cassava starch (biopolymer), the synthetic hectorite commercialized as Laponite RD®, and inverted sugar as plasticizer. Studies about composites of cassava starch and other materials have produced films with interesting properties.[41-43]

Cassava-Laponite nanocomposites were prepared by solvent-assisted process in which clay is previously dispersed in water. Afterwards, colloidal dispersion of clay particles is added to the aqueous dispersion containing the biopolymer and inverted sugar as plasticizer (Fig. 1B). Cassava-Laponite films prepared by casting were characterized by X-ray diffraction, scanning and transmission electron microscopy techniques (SEM and TEM), vibrational (Raman) spectroscopy, thermogravimetric analysis and tensile tests.

Experimental

Preparation of cassava-Laponite films

Laponite RD (from Laporte Industries, UK) was exfoliated in deionized water. The nominal cassava starch/Laponite proportions (m/m%) were 100/0, 95/5, 90/10, 85/15, 70/30, and the composites are noted as Cas-Lap (100/0), Cas-Lap (95/5), Cas-Lap (90/10), Cas-Lap (85/15), and Cas-Lap (70/30), respectively. One dispersion containing Laponite RD in 50 mL of H_2O *(dispersion 1)* and another containing cassava powder in 200 mL of H_2O *(dispersion 2)* were submitted to thermal treatment at 70 °C for 2 hours under mechanical stirring. The total of starch and clay amount was 10 g in each film. Dispersion 1 was added slowly on the dispersion 2 and, concomitantly, 1.2 mL (1.5 g) of inverted sugar cane syrup

(from Copersucar Industries, Brazil) was added. After the addition, the obtained mixture was maintained under thermal treatment at 70 °C for 30 min under stirring. A volume of 85 mL of the obtained gel was poured in plastic recipients of 12 cm diameter. The gels were dried at 70 °C for 12 h in an oven under reduced pressure. After drying, the films were conditioned for 96 h in a closed box containing a saturated solution of KCl (85% relative humidity) and later kept in Zip-Lock bags to avoid humidity changes.

Characterization of starch-clay hybrid materials

X-ray diffraction (XRD) patterns were recorded in a Rigaku diffractometer, model Miniflex, using Cu-K_α radiation (1.541 Å, 30 kV and 15 mA) and Ni filter. The step used was 0.02 ° *per* second in the angular domain (2θ) 2-70 °.

Fourier transformed Raman spectra (FT-Raman) were recorded in an FT-Raman Bruker FRS-100/S spectrometer using 1064 nm exciting radiation (Nd:YAG laser Coherent Compass 1064-500N) and a Ge detector. Laser power was kept below 20 mW to avoid sample degradation. FT-Raman spectra of Cas-Lap films were baseline corrected.

Mass coupled thermogravimetric analysis (TGA-MS) were recorded on a Netzsch equipment model TGA/DSC 490 PC Luxx coupled to an Aëolos 403C mass-spectrometer, using a heating rate of 10 °C min^{-1} and both synthetic air and nitrogen flow of 50 mL min^{-1}.

Field emission scanning electron microscopy (FE-SEM) images of uncoated samples were obtained in a JEOL microscope, model JSM-7000F, at the Instituto de Química (Universidade de São Paulo - USP). Transmission electron microscopy (TEM) images were recorded on a 300 kV JEM-3010 ARP microscope at the LNNano - CNPEM (Center for Nanoscience and Nanotechnology/ MCT, Campinas, Brazil). Samples for the TEM images were prepared by dispersing the solids in propanol in an ultrasonic bath followed by deposition on a carbon-coated Cu microgrid.

A texture analyzer TA-XT2i (Stable Micro System, England) equipped with A/TGT probe roller grips for extensibility accessory was used to measure the extensibility and resistance to extension of starch films. The procedure was based on the ASTM D 882-02. Rectangular pieces of 20 × 80 × 0.1 mm^3 were tested under extensibility at 0.8 mm s^{-1} rate and l_0 = 10 mm until rupture. The samples were tested at 50% relative humidity.

Results and Discussion

Amylose is responsible for the film-forming capacity of starch based films[44] due to its higher tendency to interact through hydrogen bonds and therefore, generating stiffer and stronger films when compared to amylopectin.[45] Extensive intermolecular forces among polymer chains are responsible for the brittleness of starch-based films.[46,47] Hence, the addition of a plasticizing agent is a necessary feature in this system in order to overcome the intrinsic brittleness of starch films. The strong interfacial interaction between the biopolymer and clay is evidenced for homogeneous gels and films formed.

XRD patterns of the nanocomposites are shown in Figure 3. XRD pattern of pristine starch granules shows several peaks over the region (2θ) 15-25 ° due to its hierarchical organization of branched polymer amylopectin along the granule.[32] The set of peaks at (2θ) 15.2, 17.2, 18.1 and 23.1 ° is characteristic of a monoclinic packing structure of the double helices of amylopectin, known as A-pattern.[38] On the other hand, XRD patterns of Cas-Lap (100/0) and Cas-Lap (95/5) films (Figure 3b and 3c) show the presence of small peaks in the range between 14.6 and 26.0 °, related to the semi-crystalline organization of pristine starch granules, indicating that the conditions employed to prepare these materials were not enough to completely break its organizational level.

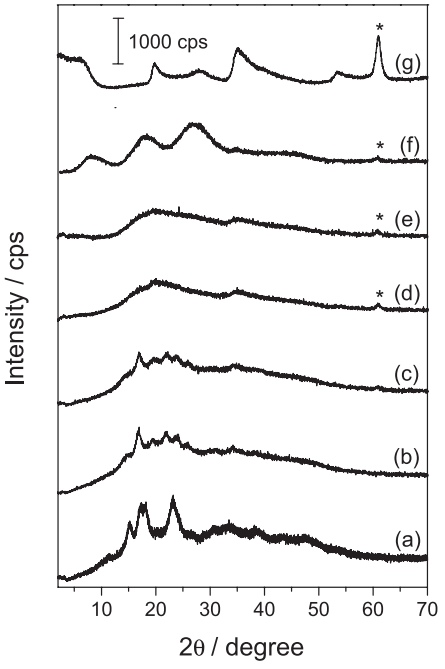

Figure 3. XRD patterns of (a) cassava starch granules (powder) and the films (b) Cas-Lap (100/0), (c) Cas-Lap (95/5), (d) Cas-Lap (90/10), (e) Cas-Lap (85/15), (f) Cas-Lap (70/30) and (g) Laponite RD. (*) (060/330) peak diffraction of Laponite clay.

During the gelatinization process in water-based systems, the first event is related to the granule swelling by water uptake, especially in the amorphous regions of the granule. Later, starch granule begins to solubilize,

releasing amylose chains in a non-reversible reaction.[48,49] When the temperature in the system increases even further, the chains from starch polymers reduce drastically the side interactions among double helices, allowing the unwinding of amylopectin chains as a final process of gelatinization.[50] The transition from pristine starch suspension to a gel-like solution can be noticed by the fading of the white suspension followed by a viscous pearly solution that takes place once the rupture of the granules is initiated. Small amounts of clay do not promote structural changes in the polymeric film, since XRD profile of the Cas-Lap (95/5) film (Figure 3c) is very similar to Cas-Lap (100/0) film (Figure 3b).

XRD patterns of Cas-Lap (90/10) and Cas-Lap (85/15) films show a decrease in the crystallinity of the polymer when compared to the sample Cas-Lap (95/5) due to the absence of the peaks associated with the granular phase. When the clay loading is higher than 5%, a peak at (2θ) 61° (overlapped (060) and (330) planes; signal marked with asterisk)[22] indicates the presence of the Laponite clay. The occurrence of this peak might be only noticeable at higher clay concentration due to a concentration effect. The absence of a peak related to intercalation (d_{001}) indicates the obtaining of preferentially exfoliated hybrid materials.[51] On the other hand, the XRD pattern of Cas-Lap (70/30) sample (Figure 3f) exhibits several basal reflections (00*l*), indicating an ordered layered structure. Taking into account the basal spacing of 1.35 nm (calculated from d_{001} peak) and the clay layer thickness (0.96 nm), the interlayer distance (about 0.4 nm) suggest the intercalation process of polymer chains into the interlayer domain. Considering only the XRD data, it is not possible to evaluate the extension of formation of an intercalated or exfoliated material.

FT-Raman spectra of Cas-Lap films are shown in Figure 4; spectra of cassava starch granules (Figure 4a) and of Laponite (Figure 4g) are shown for comparison purposes. Raman spectrum of cassava starch granules is very similar to the previous ones reported of starches from different sources confirming the presence of amylose and amylopectin in these films.[52,53]

Laponite FT-Raman spectrum presents only one intense band at 683 cm^{-1} assigned to tetrahedral [SiO_4] lattice mode.[54] The band at 683 cm^{-1} is observed in nanocomposites with higher amount of clay indicating the presence of Laponite layers in these samples. The bands at 480 and 940 cm^{-1} are assigned to skeletal vibrations of the pyranose ring and to the glycosidic linkage, respectively; these bands remain nearly constant in all Cas-Lap films. In contrast, the set of bands from 1200-1400 cm^{-1} assigned to CH_2 scissoring and CH_2 twisting[55] become broader as the amount of Laponite is increased. Indeed, these bands were reported

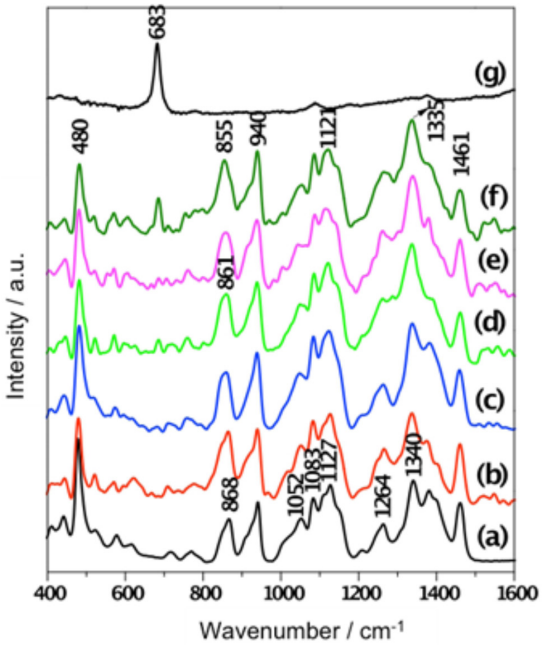

Figure 4. Raman spectra of (a) cassava starch granules, (b) Cas-Lap (100/0), (c) Cas-Lap (95/5), (d) Cas-Lap (90/10), (e) Cas-Lap (85/15), (f) Cas-Lap (70/30) and (g) Laponite RD.

being particularly sensitive to hydrogen bonding with other molecules.[56] As the Laponite amount is increased, the bands at 1127 cm^{-1} (C–O stretching and C–O–H bending), 868 cm^{-1} (C–H deformation) and 1340 cm^{-1} (C–H wagging) in cassava starch granules are progressively shifted to lower wavenumbers; for Cas-Lap 70/30 these bands are observed at 1121, 855 and 1335 cm^{-1} respectively. This shift was reported in the gelatinization process where crystalline structure of starch is converted to gel particles by action of heat.[57] These results indicate that starch in Cas-Lap is progressively less crystalline as the amount of Laponite is increased in agreement with XRD data.

The representative SEM images of cassava starch granules and nanocomposites materials are shown in Figure 5. The morphology of cassava starch reveals its granular nature, while all the films obtained lose this type of organization due to the starch gelatinization process. All the resulting films show high homogeneity and transparency, even at high content of clay, evidencing strong interaction between the clay and the biopolymer. The analyzed films are also free of aggregates that could possibly arise from the condensation of a large number of clay platelets.

Figure 6 shows TEM images registered at different portions of the nanocomposite with the high Laponite content (Cas-Lap 70/30). The small dark fringes observed in the images (region identified with a circle in Figure 6a and with arrows in Figure 6c) are attributed to clay particles dispersed on the biopolymer. It is possible to observe that most of these clay particles are mainly

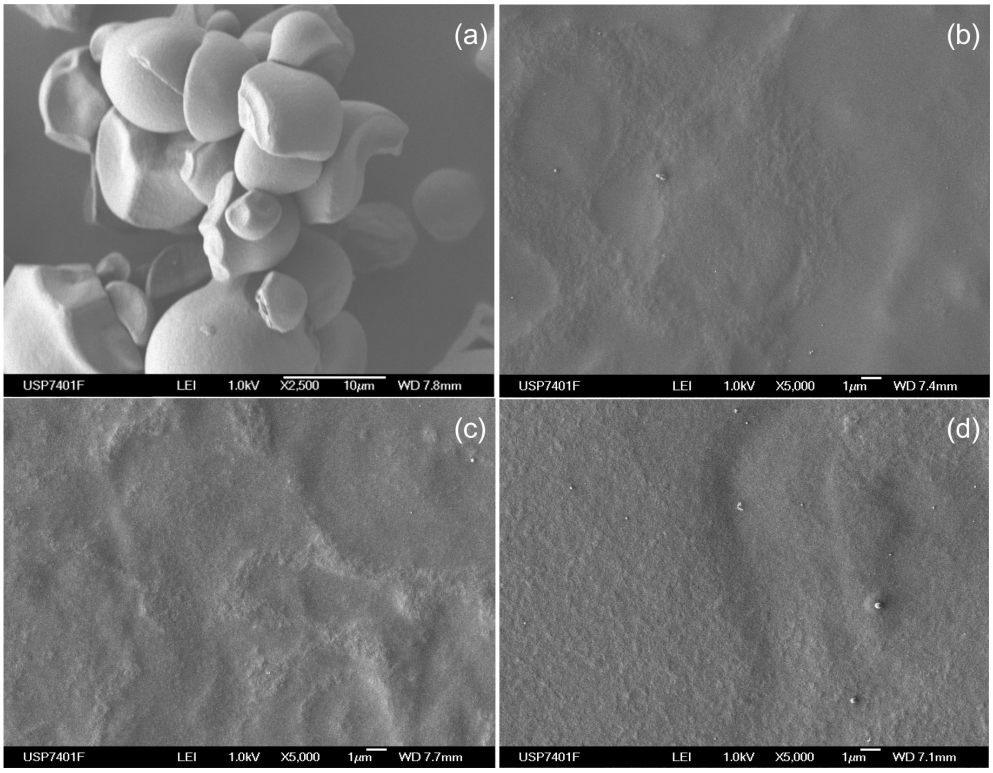

Figure 5. SEM images of (a) cassava starch granules, (b) Cas-Lap (100/0), (c) Cas-Lap (95/5) and (d) Cas-Lap (70/30).

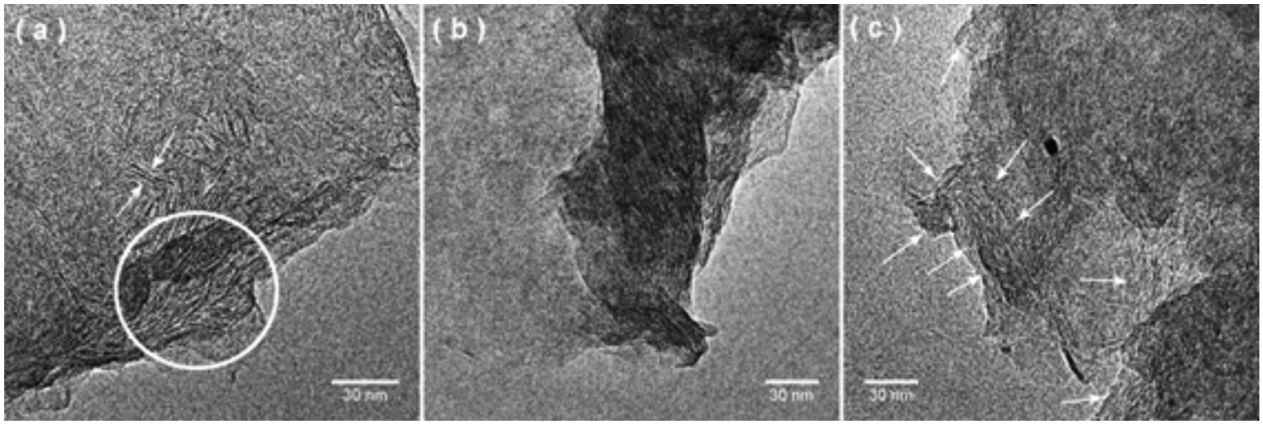

Figure 6. TEM images of the nanocomposite Cas-Lap (70/30).

concentrated at the edges of the nanocomposite. Phase segregation is not observed in TEM images, even in the regions with high clay particles amount as show in Figure 6b, indicating a good compatibility between the inorganic and organic phases.

The absence of long distance ordering of the clay particles in the biopolymer is observed in Figures 6a and 6c, where the silicate layers appear to exist as single and double layers (exfoliated nanocomposite). A fraction of stacked platelets (intercalated nanocomposite) is also observed in the Cas-Lap (70/30) film (Figure 6b). Using the ImageJ software,[58] the thickness of exfoliated layers and the distance between two platelets were determined respectively as around 0.6 nm and 1.6 nm. This measurement was performed in fringes indicated by two-faced white arrows in Figure 6a. The distance between the double layers (1.6 nm) is in accordance to the results observed in X-ray diffraction pattern (Figure 3f) as it is expect to represent the basal spacing of the intercalated nanocomposite.

The thermogravimetric curves of the nanocomposites under air atmosphere are presented in Figure 7. The profiles of the curves for cassava starch granules and Cas-Lap (100/0) are very similar (Figures 7a and 7b); both materials present three main steps of thermal decomposition. The first step corresponds to the release of adsorbed water molecules

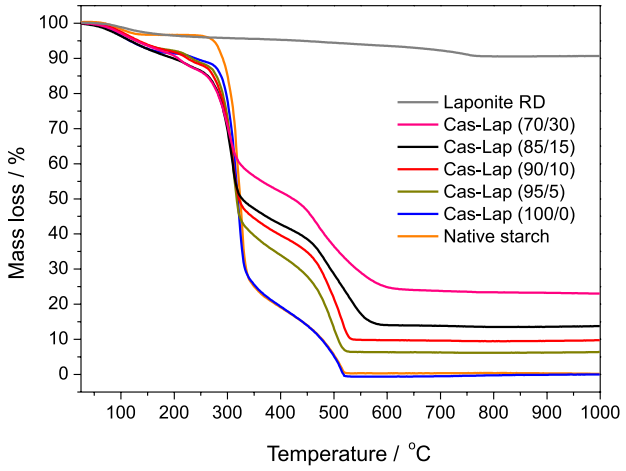

Figure 7. TGA curves of cassava starch granules (blue), Cas-Lap (100/0) (orange), Cas-Lap (95/5) (green), Cas-Lap (90/10) (red), Cas-Lap (85/15) (black), Cas-Lap (70/30) (pink) and Laponite RD (grey).

and the event occurs from room temperature to 135 °C for cassava starch granules and until 250 °C for Cas-Lap, as confirmed by DTG-MS curves of m/z = 18 assigned to water release (Figure 8).

The mass loss in this temperature range was 3.3 wt.% for cassava starch granules and 11.9 wt.% for the starch film without clay. For the nanocomposites Cas-Lap (95/5), Cas-Lap (90/10), Cas-Lap (85/15), and Cas-Lap (70/30), the weight loss associated with the water molecules release is around 13 wt.%. For the Cas-Lap (100/0) film, the second and third steps of decomposition occur between 250 °C and 580 °C with water vapor (m/z = 18), CO_2 (m/z = 44) and CO (m/z = 28) release due to the biomolecule decomposition (Figure 8a). No significant shift towards higher temperatures in the second event of mass loss was observed as clay load is increased. The mass loss of these two mentioned events varies according to the clay content ranging from 75 wt.% to 40 wt.%. The residue content also varies with the clay loading, from 6.7 wt.% to 23.2 wt.%.

In the clay composite materials, in addition to the biopolymer decomposition, in the second and third steps, the partial dehydroxylation of Laponite sheets also takes place. According to Malek *et al.*,[59] for the pristine Laponite, above 600 °C exchangeable cations migrate into the silicate layer and the clay structure is collapsed. In the case of Cas-Lap (70/30) composite (Figure 8d), host inorganic structure increases the thermal stability of the organic biomolecule guest in relation to the unmodified biopolymer. The thermal decomposition of the organic biomolecules, when clay content is high, alters considerably the proportion of released CO_2 in the second and third steps promoting the formation of more CO_2 only with increase of temperature (Figure 8d).

Figure 9 shows the TGA curves of nanocomposite Cas-Lap (95/5) in both synthetic air and nitrogen curves. Up to 320 °C, the nanocomposite shows a similar thermal behavior and therefore, it is possible to conclude that the first process of decomposition of polymeric structure

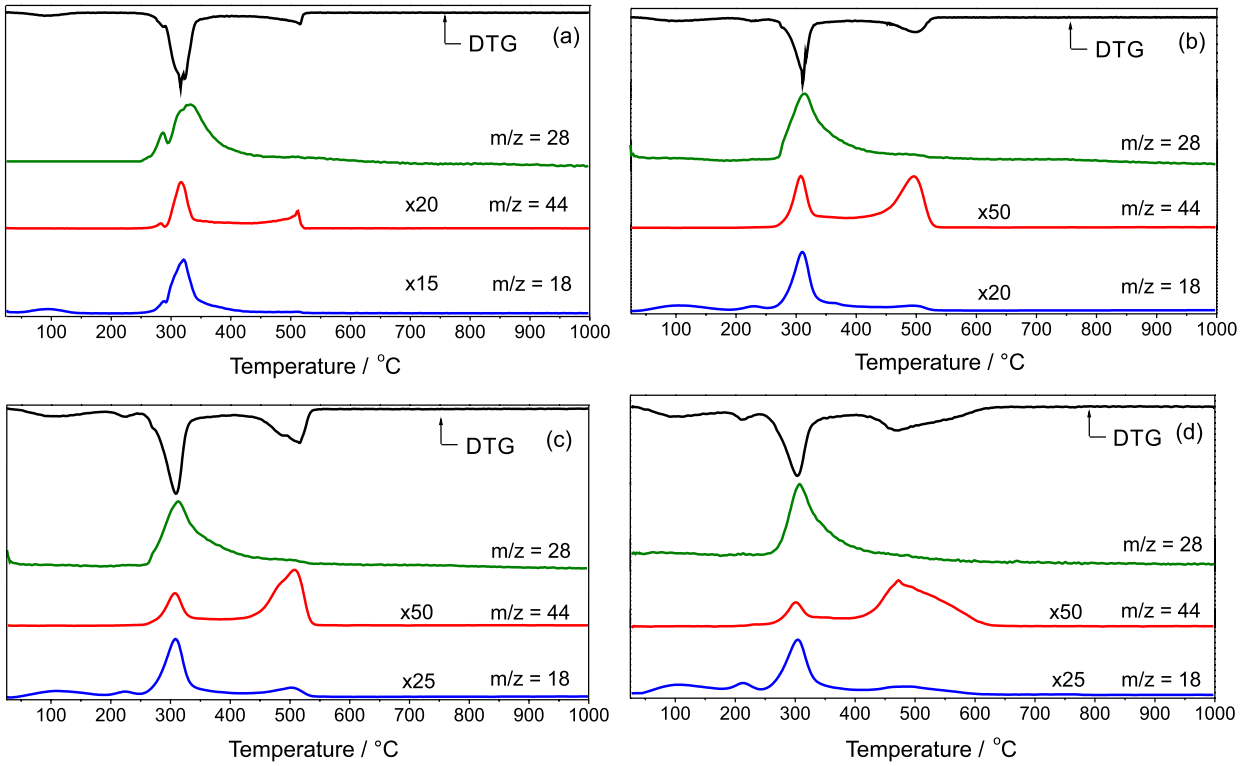

Figure 8. DTG-MS curves of: (a) cassava starch granules, (b) Cas-Lap (100/0), (c) Cas-Lap (90/10) and (d) Cas-Lap (70/30).

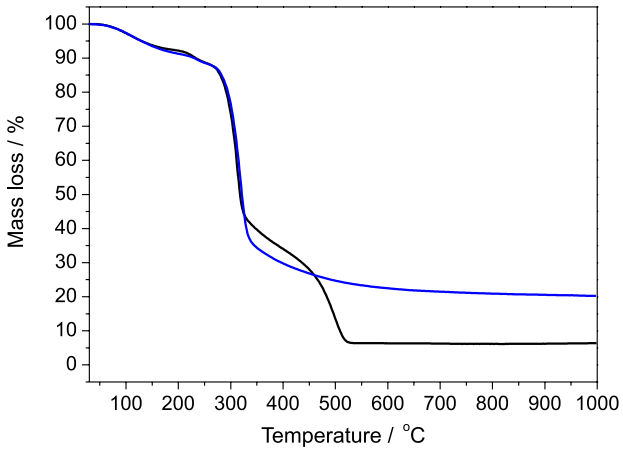

Figure 9. TGA curves for Cas-Lap (95/5) nanocomposite under synthetic air (black) and nitrogen atmosphere (blue).

undergoes by a non-oxidative process, generating fragments arising from parts of the glucopyranose chains.

It is noticed a slight decrease in the mass loss process for the nanocomposite from 320 to 500 ºC under nitrogen atmosphere. When using synthetic air, it is observed another decomposition step from 300 to 500 ºC, associated to the oxidation of the remaining carbonaceous residue generated in the previous non-oxidative step, evidenced by the byproducts of decomposition in this range, mainly constituted of water (m/z = 18) and carbon dioxide (m/z = 44), as seen in Figure 10.

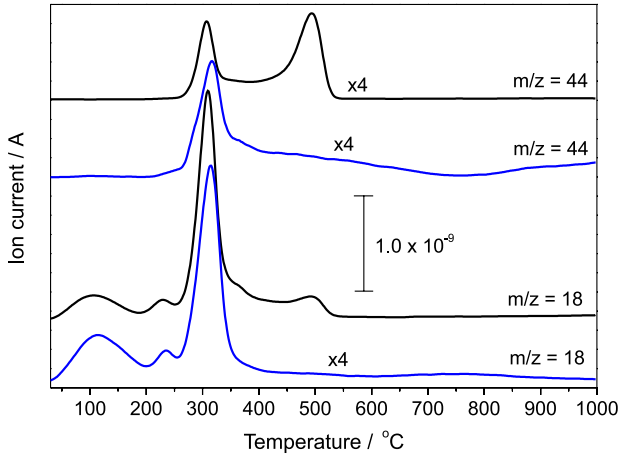

Figure 10. MS curves for the fragments m/z = 18 and m/z = 44 for the Cas-Lap (95/5) under synthetic air atmosphere (black) and nitrogen atmosphere (blue).

The profiles of the main evolved gases detected in both atmospheres for the nanocomposite Cas-Lap 95/5 are shown in Figure 11. It should be considered, however, that the detected curve of carbon monoxide, for both atmospheres, was not included due to the contribution of N_2 gas for the total intensity of the fragment m/z = 28.

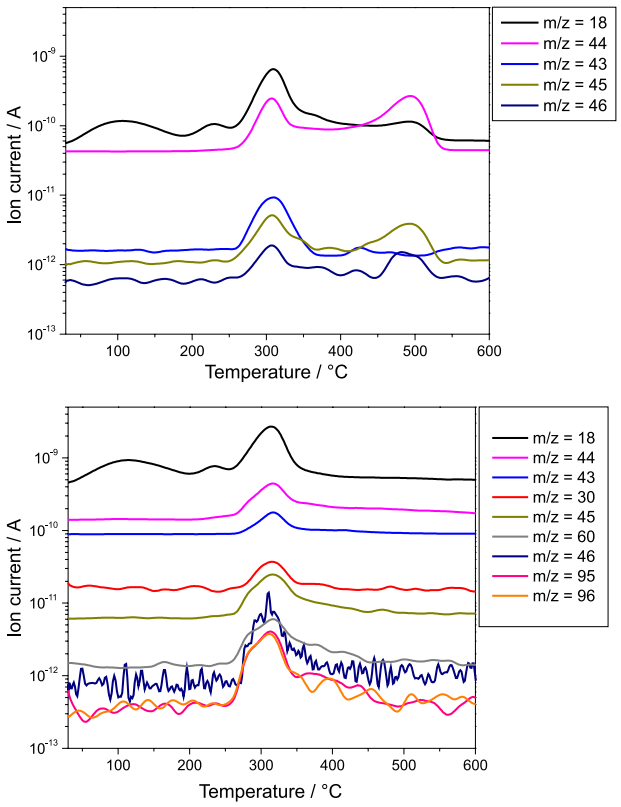

Figure 11. Detected fragments for the Cas-Lap (95/5) nanocomposite under synthetic air atmosphere (top) and under nitrogen atmosphere (bottom).

Due to the lack of an oxidizing agent in the nitrogen atmosphere, it is observed a larger number of detected fragments, in comparison to the synthetic air atmosphere, as shown in Figure 11. For the first case, the most intense secondary fragments detected (in addition to water, carbon monoxide and carbon dioxide) were formaldehyde (m/z = 30), formic acid (m/z = 46), acetic acid and its fragments (m/z = 60, m/z = 43, m/z = 47) and furfural and its fragments (m/z = 96, m/z = 95). It was also observed that the increase of clay content in the nanocomposite causes a significant drop in the intensity of the secondary fragments in a higher scale than expected for only the reduction of the polymeric content. This fact suggests that at high concentration, even under inert atmosphere, clay particles can act as a catalyst for the thermal decomposition of the polymer, generating as byproducts fragments with low molecular masses.

The results of tensile tests for the obtained materials are show in Figure 12. The data with mean values and statistical analysis of maximum tensile strength, maximum elongation and Young's modulus are shown in Table 1. The sample without clay, Cas-Lap (100/0), shows the highest elongation at break than the other nanocomposites even though it shows the lowest strength among the entire set of

Table 1. Mechanical parameters of cassava starch-based nanocomposites

Sample	Tensile strength / MPa	Maximum elongation / %	Young's modulus / GPa
Cas-Lap (100/0)	6.54 ± 0.80[a]	48.01 ± 3.98[a]	1.28 ± 0.42[a]
Cas-Lap (90/10)	18.79 ± 0.64[b]	5.90 ± 0.24[b]	5.07 ± 0.68[b]
Cas-Lap (70/30)	18.13 ± 0.61[b]	4.02 ± 0.15[b]	7.11 ± 0.80[c]

Same lower case letters (a,b,c) for a given parameter are not statistically different at $\alpha = 0.05$ - Tukey's honest significant test.

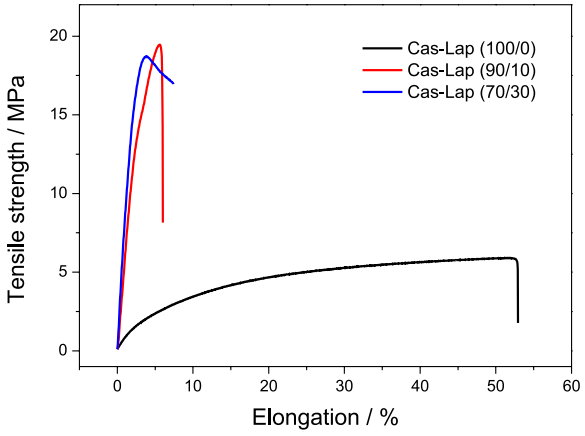

Figure 12. Tensile tests of Cas-Lap (100/0) (black), Cas-Lap (90/10) (red) and Cas-Lap (70/30) (blue).

analyzed materials. As it can be observed, the increase of clay content affects directly all the mechanical parameters analyzed.

The tensile strength is enhanced by a factor of almost three times when clay is added to the polymer system in comparison to the thermoplastic starch. This phenomenon occurs due to the nanoscale interaction of both organic and inorganic phases through establishment of hydrogen bonds, increasing the necessary force to promote the slippage of the polymer chains.[60] At the same time, since the slippage of the chains is hindered by the interaction between both phases, it is observed a great reduction in the maximum elongation when clay is added to the polymer. Young's modulus was the only parameter found to be statistically different for each of three samples analyzed. In this case, it was observed that an increase of clay content in the nanocomposite led to an increase in the modulus of elasticity. This result can be explained regarding an increase of the interface of interaction between both phases as clay content in the nanocomposite is increased. It can also be inferred that for materials with clay content higher than 10 wt.%, no substantial benefit for either elongation or resistance is achieved. Future studies should be made exploring the intermediate region of the graphic in order to obtain materials with balanced elongation/strength.

Conclusions

PCN materials based on synthetic hectorite clay and cassava starch were prepared. When small amounts of clay are added, the XRD data indicate the formation of mostly exfoliated nanocomposites, in which individual or few stacked inorganic layers are dispersed in the polymer matrix. On the other hand, when great amounts of clay are added, the intercalated nanocomposites are mostly formed. FT-Raman spectra indicate that crystallinity of starch in the hybrid films decreases as the amount of Laponite is increased, corroborating with XRD data. Prepared films are transparent and homogeneous. According to TGA analysis, the different steps of thermal decomposition are dependent on the amount of clay in the hybrid material. The good dispersion of Laponite particles in the biodegradable starch polymer is attractive to develop functional materials for nanomedicine applications.

Acknowledgements

The authors are indebted to the Brazilian agencies Fapesp (Fundação de Amparo à Pesquisa do Estado de São Paulo, project 2011/50318-1), CNPq (Conselho Nacional de Desenvolvimento Científico e Tecnológico), and Nanobiomed (Nanomedicine Network/CAPES) for financial support and fellowships. We also appreciate the support from C2NANO - Center for Nanocience and Nanotechnology/MCT, and NAP-NN (Núcleo de Apoio à Pesquisa em Nanossistemas e Nanotecnologia) from Universidade de São Paulo.

References

1. Xu, W.; Zeng, Q.; Yu, A.; *Polymer* **2012**, *53*, 3735.
2. Alexandre, M.; Dubois, P.; *Mater. Sci. Eng. R-Rep.* **2000**, *28*, 1.
3. Okada, A.; Usuki, A.; *Macromol. Mater. Eng.* **2006**, *291*, 1449.
4. Kato, M.; Usuki, A.; Hasegawa, N.; Okamoto H.; Kawasumi, M.; *Polym. J.* **2011**, *43*, 583.
5. Ray, S. S.; Okamoto, M.; *Prog. Polym. Sci.* **2003**, *28*, 1539.
6. Nascimento, G. M.; Constantino, V. R. L.; Landers, R.; Temperini, M. L. A.; *Macromolecules* **2004**, *37*, 9373.

7. Sanchez, C.; Belleville, P.; Popall, M.; Nicole, L.; *Chem. Soc. Rev.* **2011**, *40*, 696.
8. Shchipunov, Y.; *Pure Appl. Chem.* **2012**, *84*, 2579.
9. Ray, S. S.; Yamada, K.; Okamoto, M.; Ogami A.; Ueda, K.; *Chem. Mater.* **2003**, *15*, 1456.
10. Maiti, P.; Batt C. A.; Giannelis, E. P.; *Polym. Mater. Sci. Eng.* **2003**, *88*, 58.
11. Kiliaris, P.; Papaspyrides, C. D.; *Prog. Polym. Sci.* **2010**, *35*, 902.
12. Park, H. M.; Liang, X.; Mohanty, A. K.; Misra, M.; Drzal, L. T.; *Macromolecules* **2004**, *37*, 9076.
13. Choudalakis, G.; Gotsis, A. D.; *Eur. Polym. J.* **2009**, *45*, 967.
14. Darder, M.; Colilla, M.; Ruiz-Hitzky, E.; *Chem. Mater.* **2003**, *15*, 3774.
15. Laporte Absorbents; *Laponite – Structure, chemistry and relationship to natural clays*, Laponite technical bulletin L104/90/A; Laporte Absorbents: Cherise, UK, 1990.
16. http://www.byk.com/fileadmin/byk/additives/product_groups/rheology/former_rockwood_additives/technical_brochures/consumercare_brochure.pdf accessed in July 2013.
17. Gaharwar, A. K.; Mihaila, S. M.; Swami, A.; Patel, A.; Sant, S.; Reis, R. L.; Marques, A. P.; Gomes, M. E.; Khademhosseini, A.; *Adv. Mater.* **2013**, *25*, 3329.
18. Kaviratna, P. D.; Pinnavaia, T. J.; Schroeder, P. A.; *J. Phys. Chem. Solids* **1996**, *57*, 1897.
19. Shahin, A.; Joshi, Y. M.; *Langmuir* **2012**, *28*, 15674.
20. Nobel, M. L.; Picken, S. J.; Mendes, E.; *Prog. Org. Coat.* **2006**, *58*, 96.
21. Herrera, N. N.; Letoffe, J. M.; Putaux, J. L.; David, L.; Bourgeat-Lami, E.; *Langmuir* **2004**, 20, 1564.
22. Brindley, G. W. In *Crystal Structures of Clay Minerals and Their X-Ray Identification*; Brindley, G. W.; Brown, G., eds.; Mineralogical Society: London, UK, 1980, ch. 2.
23. Brigatti, M. F.; Galan, E.; Theng, B. K. G. In *Handbook of Clay Science*; Bergaya, F.; Theng, B. K. G.; Lagaly, G., eds.; Elsevier: Oxford, UK, 2006, ch. 2.
24. Kloprogge, J. T.; *J. Porous Mater.* **1998**, *5*, 5.
25. Darder, M.; Aranda, P.; Ruiz-Hitzky, E.; *Adv. Mater.* **2007**, *19*, 1309.
26. Pandey, J. K.; Kumar, A. P.; Misra, M.; Mohanty, A. K.; Drzal, L. T.; Singh, R. P.; *J. Nanosci. Nanotech.* **2005**, *5*, 497.
27. Svagan, A. J.; Åkesson, A.; Cárdenas, M.; Bulut, S.; Knudsen, J. C.; Risbo, J.; Plackett, D.; *Biomacromolecules* **2012**, *13*, 397.
28. D'Amico, D. A.; Manfredi, L. B.; Cyras, V. P.; *J. Appl. Polym. Sci.* **2012**, *123*, 200.
29. Hong, S. I.; Lee, J. H.; Baw, H. J.; Koo, S. Y.; Lee, H. S.; Choi, J. H.; Kim, D. H.; Park, S. H.; Park, H. J.; *J. Appl. Polym. Sci.* **2011**, *119*, 2742.
30. Viseras, C.; Cerezo, P.; Sanchez, R.; Salcedo, I.; Aguzzi, C.; *Appl. Clay Sci.* **2010**, *48*, 291.
31. Si-Shen, F.; Lin, M.; Panneerselvan, A.; CheeWee, G.; Zhou, W.; *Biomaterials* **2009**, *30*, 3297.
32. Gallant, D. J.; Bouchet, B.; Baldwin, P. M.; *Carbohydr. Polym.* **1997**, *32*, 177.
33. Wang, T. L.; Bogracheva, T. Y.; Hedley, C. L.; *J. Exp. Bot.* **1998**, *49*, 481.
34. Laohaphatanaleart, K.; Piyachomkwan, K.; Sriroth, K.; Bertoft, E.; *Int. J. Biol. Macromol.* **2010**, *47*, 317.
35. Buléon, A.; *Véronèse*, G.; Putaux, J. L.; *Austr. J. Chem.* **2007**, *60*, 706.
36. Parker, R.; Ring, S. G. In *Polysaccharides: Structural Diversity and Functional Versatility*; Dumitriu, S., ed.; Marcel Dekker Inc.: New York, USA, 2005, ch. 24.
37. Jane, J. L. In *Chemical and Functional Properties of Food Saccharides*; Tomasik, P., ed.; CRC Press: Boca Raton, USA, 2004, ch. 7.
38. Jiping, P.; Shujun, W.; Jinglin, Y.; Hongyan, L.; Jiugao, Y.; Wenyuan, G.; *Food Chem.* **2007**, *105*, 989.
39. http://faostat.fao.org/site/567/default.aspx#ancor accessed in July 2013.
40. Veiga-Santos, P.; Oliveira, L. M.; Cereda, M. P.; Scamparini, A. R. P.; *Food Chem.* **2007**, *103*, 255.
41. Woehl, M. A.; Canestraro, C. D.; Mikowski, A.; Sierakowski, M. R.; Ramos, L. P.; Wypych, F.; *Carbohydr. Polym.* **2010**, *80*, 866.
42. Rouilly, A.; Rigal, L.; Gilbert, R. G.; *Polymer* **2004**, *45*, 7813.
43. Teixeira, E. M.; Pasquini, D.; Curvelo, A. A. S.; Corradini, E.; Belgacem, M. N.; Dufresne, A.; *Carbohydr. Polym.* **2009**, *78*, 422.
44. Liu, Z.; Han, J. H.; *J. Food Sci.* **2005**, *70*, E31.
45. López, O. V.; Garcia, M. A.; Zaritzky, N. E.; *Carbohydr. Polym.* **2008**, *73*, 573.
46. Bertuzzi, M. A.; Vidaurre, E. F. C.; Armada, M.; Gottifredi, J. C.; *J. Food Eng.* **2007**, *80*, 972.
47. Koskinen, M.; Suortti, T.; Autio, K.; Myllärinen, P.; Poutanen, K.; *Ind. Crops Prod.* 1996, *5*, 23.
48. Vandeputte, G. E.; Derycke, V.; Geeroms, J.; Delcour, J. A.; *J. Cereal Sci.* **2003**, *38*, 53.
49. Tester, R. F.; Morrison, W. R.; *Cereal Chem.* **1990**, *67*, 551.
50. Ratnayake, W. S.; Jackson, D. S.; *Carbohydr. Polym.* **2007**, 67, 511.
51. According to the Clay Minerals Society, *"in clay science, exfoliation involves a degree of separation of the layers of a host structure where units, either individual layers or stacking of several layers, are isotropically dispersed (freely oriented and independent) in a solvent or polymer matrix."* http://www.clays.org/GLOSSARY/ClayTermsMay2013.pdf accessed in October 2013.
52. Kizil, R.; Irudayaraj, J.; Seetharaman, K.; *J. Agric. Food Chem.* **2002**, *50*, 3912.

53. Fechner, P. M.; Wartewig, S.; Kleinebudde, P.; Neubert, R. H. H.; *Carbohydr. Res.* **2005**, *340*, 2563.
54. Bishop, J. L.; Murad, E.; *J. Raman Spectrosc.* **2004**, *35*, 480.
55. Cerchiaro, G.; Sant'Ana, A. C.; Temperini, M. L. A.; Ferreira, A. M. C.; *Carbohydr. Res.* **2005**, *340*, 2352.
56. Kacuráková, M.; Mathlouthi, M.; *Carbohydr. Res.* **1996**, *284*, 145.
57. Schuster, K. C.; Ehmoser, H.; Gapes, J. R.; Lend, B; *Vib. Spectrosc.* **2000**, *22*, 181.
58. Rasband, W. S.; *ImageJ*; U. S. National Institutes of Health, Bethesda, Maryland, USA, 1997-2013, http://imagej.nih.gov/ij/.
59. Malek, Z.; Balek, V.; Garfinkel-Shweky, D.; Yariv, S.; *J. Thermal Anal.* **1997**, *48*, 83.
60. LeBaron, P. C.; Wang, Z.; Pinnavaia, T. J.; *Appl. Clay Sci.* **1999**, 15, 11.

Submitted: August 13, 2013
Published online: December 17, 2013

FAPESP has sponsored the publication of this article.